miR-431-5p Regulates Apoptosis of Cardiomyocytes After Acute Myocardial Infarction via Targeting Selenoprotein T

Haihua GENG[1], Lihua CHEN[1], Yamin SU[1], Qian XU[1], Mengkang FAN[1], Rong HUANG[1], Xiaofei LI[1], Xiaochen LU[1], Min PAN[1]

[1]Department of Cardiology, Affiliated Hospital of Nantong University, Nantong, China

Received March 19, 2021
Accepted October 5, 2021
Epub Ahead of Print January 19, 2022

Summary

Acute myocardial infarction (AMI) represents the acute manifestation of coronary artery disease. In recent years, microRNAs (miRNAs) have been extensively studied in AMI. This study focused on the role of miR-431-5p in AMI and its effect on cardiomyocyte apoptosis after AMI. The expression of miR-431-5p was analyzed by quantitative real-time PCR (qRT-PCR). By interfering with miR-431-5p in hypoxia-reoxygenation (H/R)-induced HL-1 cardiomyocytes, the effect of miR-431-5p on cardiomyocyte apoptosis after AMI was examined. The interaction between miR-431-5p and selenoprotein T (SELT) mRNA was verified by dual-luciferase reporter assay. Cell apoptosis was determined by terminal deoxynucleotidyl transferase dUTP nick end labeling (TUNEL) assay and flow cytometry. Cell viability was examined by 3-(4,5)-dimethylthiahiazo(-z-y1)-3,5-di-phenytetrazoliumromide (MTT) assay. The results of qRT-PCR showed that the expression of miR-431-5p in AMI myocardial tissues and H/R-induced HL-1 cardiomyocytes was significantly increased. After interfering with miR-431-5p, the expression of SELT in HL-1 cells was up-regulated, cell apoptosis was decreased, cell viability was increased, and lactate dehydrogenase (LDH) activity was decreased. The dual-luciferase reporter assay confirmed the targeting relationship between miR-431-5p and SELT1 3′ untranslated region (UTR). In H/R-induced HL-1 cells, the simultaneous silencing of SELT and miR-431-5p resulted in a decrease of Bcl-2 expression, an increase of Bax expression, and an increase of cleaved-caspase 3 expression compared with silencing miR-431-5p alone. Also, cell viability was decreased, while LDH activity was increased by the simultaneous silencing of SELT and miR-431-5p. Interfering miR-431-5p protected cardiomyocytes from AMI injury *via* restoring the expression of SELT, providing new ideas for the treatment of AMI.

Key words

miR-431-5p • Acute myocardial infarction • Cardiomyocyte apoptosis • Selenoprotein T

Corresponding author

M. Pan, Department of Cardiology, Affiliated Hospital of Nantong University, 20 Xisi Road, Nantong 226001, People's Republic of China. E-mail: panminmd@163.com

Introduction

Acute myocardial infarction (AMI) is one of the most serious coronary heart diseases, which causes severe damage to myocardial tissues and may lead to heart failure [1-3]. Annually, AMI causes more than 4 million deaths in Europe and North Asia [4]. AMI occurs commonly due to prolonged ischemia time of myocardial tissues (an insufficient supply of blood to the heart), while myocardial ischemia occurs due to increased myocardial metabolic demand, reduced oxygen delivery to myocardial tissues through coronary circulation (hypoxia), and reduced nutrients [5]. Therefore, the regulation of hypoxia-induced myocardial injury and its underlying molecular mechanism is of great significance in AMI.

It has been confirmed that cardiomyocyte apoptosis may be the cause of massive death of cardiomyocytes during AMI and the cause of the gradual loss of viable cells in the failing heart [6]. Previous

studies have shown that inhibiting cardiomyocyte apoptosis attenuates cardiac remodeling and heart failure after AMI [7-9]. Wang *et al.* [10] found that protein arginine methyltransferase 4 (PRMT4) deficiency increases the expression of the anti-apoptotic protein Bcl-2 and decreases the expression of the pro-apoptotic markers cleaved-caspase 3 and Bax, thereby improving left ventricular function and attenuating cardiac remodeling after AMI. Selenoprotein T (SELT) is a new type of thioredoxin protease. It has been reported that SELT exerts a cytoprotective effect after cardiac ischemic injury including myocardial infarction through its redox-active catalytic site [11].

MicroRNAs (miRNAs) are a class of non-coding RNA with a length of 21-23 nucleotides. In recent years, miRNAs have been recognized as the key regulators of cardiomyocyte apoptosis [12]. It has been reported that the aberrant levels of circulating miRNAs (like miR-1, miR-133, miR-21, etc.) are involved in AMI, indicating that miRNAs can be used as diagnostic biomarkers for AMI and that they are closely related to cardiomyocyte apoptosis [13,14]. To identify the relevant miRNAs involved in AMI, we performed miRNA analysis using the NCBI Gene Expression Omnibus (GEO) database and found that miR-431-5p may be involved in AMI progression. MiR-431-5p has been reported to be involved in many diseases, including hypertension [15] and lung cancer [16]. Knocking down miR-431-5p delays Ang II-induced hypertension and reduces vascular damage in mice [15]. These findings suggested that interfering miR-431-5p may protect cardiomyocytes from injury. Interestingly, through TargetScan database (http://www.targetscan.org/), we revealed that SELT may be one of the target genes of miR-431-5p. Therefore, we speculated that SELT may be a potential downstream target gene of miR-431-5p, and miR-431-5p can target SELT to play an essential role in cardiomyocyte apoptosis after AMI. This study aimed to explore the potential molecular mechanism of miR-431-5p in cardiomyocyte apoptosis after AMI.

Materials and Methods

Mouse model of AMI

Eight-week-old wild-type (WT) C57BL/6 J male mice were adopted to construct a mouse model of AMI as described before [17]. Mice were purchased from the Shanghai Lab Animal Research Center (Shanghai, China). All animals were group-housed under a 12 h light/dark cycle and allowed free access to food and water. Briefly, mice were anesthetized intraperitoneally with pentobarbital (60 mg/kg), and then intubated with a 22-G intravenous catheter and mechanically ventilated with a rodent respirator. The left thorax was cut in the fourth intercostal space, and the left anterior descending branch (LAD) was ligated with 8-0 silk thread about 3 mm from the tip of the left ear. When the front wall of the left ventricle turned white, the ligation was considered to be successful. The mice in the sham group were only separated the blood vessels without ligating the left anterior descending artery. Mice were divided into Sham and AMI groups with 5 in each group. All animal procedures were approved by the animal experiment ethics committee of Affiliated Hospital of Nantong University.

Microarray data

The microarray data were collected from the NCBI Gene Expression Omnibus (GEO) database (http://www.ncbi.nlm.nih.gov/geo/). Two datasets of gene chips GSE74135 and GSE76604 of myocardial infarction mice were screened by entering the keywords "(miRNA myocardial infarction) AND "Mus musculus"[porgn:__txid10090]" in the GEO database. MiRNA datasets were screened based on the selection criteria "adjusted p value <0.05". The intersection of the two datasets was taken for further analysis.

Hematoxylin and eosin (H&E) staining

The pathological changes of heart tissues were evaluated by H&E staining. A microtome was used to cut the paraffin-embedded samples into 5 mm thick serial sections. The sections were deparaffinized in xylene, rehydrated with different concentration gradients of ethanol, and stained with H&E. After fixing with xylene-based medium, the sections were examined under an optical microscope (Olympus).

Cell culture and transfection

Mouse cardiomyocyte cell line HL-1and human embryonic kidney cells 293 (HEK-293) were obtained from the Institute of Biochemistry and Cell Biology of Chinese Academy of Sciences (Shanghai, China). HL-1 cells were cultured in complete high-glucose Dulbecco's Modified Eagle's Medium (DMEM) medium. When the cells reached about a density of 90-100 % confluence, cells were washed twice with 6 ml of autoclaved 1× phosphate buffered saline (PBS) solution.

The cells were digested with 0.25 % trypsin at room temperature. And the cell suspension was collected and centrifuged at 800× g for 6 min. Then, cells were inoculated in new culture flasks at a ratio of 1:6.

For cell transfection, miR-431-5p antagomir, and its negative control (antagomir-NC), miR-431-5p agomir and its negative control (agomir-NC), and small interfering RNA (si-SELT) was designed by GenePharma (Shanghai, China). They were transfected into HL-1 cells using Lipofectamine 2000 (Invitrogen) according to the manufacturer's instructions.

Hypoxia-reoxygenation (H/R) induced HL-1 cardiomyocyte injury

Mouse cardiomyocyte cell line HL-1 was used to establish a cardiomyocyte injury model by H/R treatment. Put Simply, HL-1 cells were cultured in an incubator containing 37 °C and 5 % CO_2. HL-1 cells were sealed in a moist hypoxic chamber (BioSpherix, Lacona, NY, USA) containing 1× Esumi' s lethal ischemic medium for 3 h and then reoxygenated in 1× Esumi controlled medium with 95 % air and 5 % CO_2. Cells in the control group were incubated for 6 h in a regular medium.

Cell viability

Cell viability was determined by 3-(4,5)-dimethylthiahiazo(-z-y1)-3,5-di-phenytetrazoliumromide (MTT) assay. After H/R treatment or cell transfection, cells were washed with phenol red-free RPMI-1640 medium. MTT solution with a final concentration of 0.5 mg/ml was added to the cells, 10 µl per well. Cells were then incubated at 37 °C for 2 h. An absorbance microplate reader (BioTek, VT, USA) was applied to record the purple absorbance produced by viable cells at 560 nm and 750 nm wavelengths. The corrected absorbance value (560-750 nm) was expressed as the percentage of viable cells relative to the untreated control.

Lactate dehydrogenase (LDH) assay

HL-1 cells were seeded in a 24-well plate (2×10^5 per well). MiR-431-5p antagomir, antagomir-NC, si-SELT, and si-control were transfected into HL-1 cells, respectively. LDH activity was determined using an LDH cytotoxicity detection kit (Beyotime, Haimen, China) according to the instructions. Put simply, 1 h before the end of H/R treatment, LDH release reagent was added to the wells, and then the plates were placed in the incubator. After reaching the treatment time, the culture plate was centrifuged. And the supernatant was taken from each well. LDH detection working solution (60 µl) was applied to each well, and the mixture was incubated at room temperature for 30 min in the dark. The absorbance was measured at 490 nm.

Terminal deoxynucleotidyl transferase dUTP nick end labeling (TUNEL) assay

TUNEL assay was carried out using TUNEL detection kit (in situ cell death detection kit, POD, Roche, Germany) according to the manufacturer's instructions.

After dewaxing and rehydration, the slides were treated with 10 mmol/l proteinase K for 15 min and then immersed in the TUNEL reaction mixture at 37 ℃ in a dark, humid environment for 1 h.

Cells were fixed with freshly prepared fixative at 15-25 ℃ for 1 h. PBS solution was applied to rinse the slides. Next, the cells were incubated with blocking solution for 10 min and washed with PBS, then incubated with the permeate for 2 min.

Finally, the slides were incubated in Converter-POD for 30 min. Those with brown particles in the nucleus were TUNEL positive cells. Under the light microscope, 5 high-power lens (×400) fields were randomly selected on each slide.

Flow cytometry

The apoptosis ratio of HL-1 cells was measured using Annexin V-FITC Apoptosis Kit (BD Biosciences, San Jose, CA, USA). After treatment, HL-1 cells were collected and washed twice with PBS. Cells were then resuspended in 1× Annexin V binding buffer and added to Annexin V-fluorescein isothiocyanate (Annexin V-FITC) (5 µl) and propidium iodide (PI) (5 µl) at room temperature for 15 min. After that, the mixture was added with 400 µl of 1× binding buffer and vortexed gently. Flow cytometry was applied within 1 h. The final fluorescence of Annexin V-FITC was collected on a BD Accuri C6 Plus personal flow cytometer (BD Biosciences).

Quantitative real-time PCR (qRT-PCR)

qRT-PCR was performed to analyze gene expression in myocardial tissues or cardiomyocytes. Total RNA was extract using Trizol reagent (Invitrogen, Carlsbad, CA, USA). Subsequently, RNA was reverse transcribed into complementary deoxyribonucleic acid (cDNA) with reverse transcriptase kit (Promega). SYBR® premixed Dimer Eraser™ was used for mRNA expression analysis. The StepOne™ system (Applied Biosystems, Foster City, CA, USA) was applied for

qRT-PCR. The thermal conditions consisted of pre-denaturation at 95 ℃ for 5 min, followed by 40 cycles of denaturation at 95 ℃ for 15 s, annealing at 56 ℃ for 15 s, extension at 72 ℃ for 30 s. Primer sequences:

miR-431-5p forward:
5'-GCGGCGGTGTCTTGCAGGCCGTC-3';
reverse:
5'-ATCCAGTGCAGGGTCCGAGG-3';
SELT forward:
5'-TGTTGATGCCACCTGACTCT-3';
reverse:
5'-AACTTCCTGCTATCCGAGGAC-3';
U6 forward:
5'-CTCGCTTCGGCAGCACA-3';
reverse:
5'-GTGCAGGGTCCGAGGT-3';
GAPDH forward:
5'-TTCTGAGCTTGCCTCTTCCG-3;
reverse:
5'-GCAGCTACGGTACACTCCTC-3'.

U6 and GAPDH were used as internal controls. The relative expression of miR-431-5p and SELT mRNA was calculated by the $2^{-\Delta\Delta Ct}$ method.

Western blotting

Tissues or cells were lysed with RIPA lysis buffer (Beyotime, China) to extract total protein. The lysate was centrifuged at 12000× g for 25 min at 4 °C. The supernatant was aspirated and the protein concentration was measured with a BCA protein assay kit (Thermo Fisher Scientific, Waltham, MA). Then, the proteins were separated by 15 % SDS-polyacrylamide gel electrophoresis (SDS-PAGE) gel using an electrophoresis system. After the electrophoresis, the proteins were transferred to polyvinylidene fluoride (PVDF) membranes (Millipore, USA) at 250 mA for 90 min. After that, the membranes were blocked with 5 % skim milk at room temperature for 1 h, and then incubated with the primary antibodies against SELT (1:1000, PA5-26314, Thermo Fisher Scientific), caspase 3 (1:1000, 700182, Thermo Fisher Scientific), Bax (1:1000, 33-6400, Thermo Fisher), cleaved-caspase-3 (1:200, ab2302, Abcam, Cambridge, UK), Bcl-2 (1:50, MA5-11757, Thermo Fisher Scientific) and β-actin (1:5000, Abcam) overnight at 4 °C. The membranes and the HRP-conjugated secondary antibody were then incubated for 2 h at room temperature. The target proteins were observed using an enhanced chemiluminescence (ECL) kit (Thermo Fisher Scientific) through an ECL system.

Dual-luciferase reporter assay

Bioinformatics software (TargetScan, www.targetscan.org) was applied to predict the target genes of miR-431-5p, and dual-luciferase reporter gene assay was performed in HEK-293 cells to study the interaction between miR-431-5p and SELT. SELT 3' untranslated region (UTR) WT and SELT 3' UTR mutant (Mut) plasmids were constructed by GENERAY Biotechnology (Shanghai, China). The luciferase reporter plasmids and miR-431-5p inhibitor, miR-431-5p mimic or their corresponding negative control were co-transfected into HEK-293 cells using Lipofectamine 2000. After 48 h of transfection, Dual-Luciferase® reporter gene assay kit (Promega, Madison, WI, USA) was used to measure the luciferase activity according to the manufacturer's protocol. Luciferase activity was standardized to renilla level.

Statistical analysis

The experimental data were expressed in the form of mean ± standard deviation, and statistical analysis was performed on GraphPrism version 7.0 (GraphPad Software, CA, USA). Data were tested for normality using Normality and Lognormally Tests. For normally distributed data, Student's *t*-test or one-way analysis of variance was applied to analyze the differences between groups. For non-normally distributed data, Mann-Whitney U test or Kruskal-Wallis test was carried out. $P<0.05$ indicated that the difference between the data was statistically significant.

Results

The expression of miR-431-5p was elevated in AMI myocardial tissues and H/R-induced HL-1 cardiomyocytes

We selected two datasets of gene chips GSE74135 and GSE76604 of AMI mouse from NCBI GEO Datasets and obtained a series of miRNAs according to the screening conditions (adjusted p value <0.05). After taking the intersection, 9 miRNAs were found in both datasets. The expression of 7 miRNAs including mmu-miR-199a-5p, mmu-miR-199a-3p, mmu-mir-214, mmu-miR-337-5p, mmu-miR-34b-3p, mmu-miR-431-5p, mmu-mir-379 was up-regulated (red), and 2 miRNAs (mmu-miR-2183, mmu-mir-669i) were expressed inconsistently (yellow) (Table 1 and Fig. 1A). By consulting the literature, we found that miR-431-5p is involved in cardiovascular-related diseases [15], but has not been reported in AMI yet. While the rest 6 miRNAs are related

to AMI. Then, we established an AMI mouse model and an H/R-induced HL-1 cardiomyocyte model. The expression of miR-431-5p was measured in AMI myocardial tissues and H/R-induced HL-1 cells. Pathological sections of myocardial tissues indicated that the fibers of the Sham group were neatly arranged, with a little neutrophil infiltration. While the tissues of the AMI group had obvious cardiomyocyte necrosis, edema, and neutrophil infiltration and disorder. Observation of cardiomyocytes by fluorescence microscope indicated that there was obvious cardiomyocytes apoptosis in the area of myocardial infarction in the AMI group, but only a few cardiomyocytes in the sham group showed apoptosis (Fig. 1B). qRT-PCR results revealed that the expression of miR-431-5p in myocardial tissues of AMI mice was increased compared with the Sham group (Fig. 1C). In H/R-induced HL-1 cells, the expression of miR-431-5p was also increased (Fig. 1D).

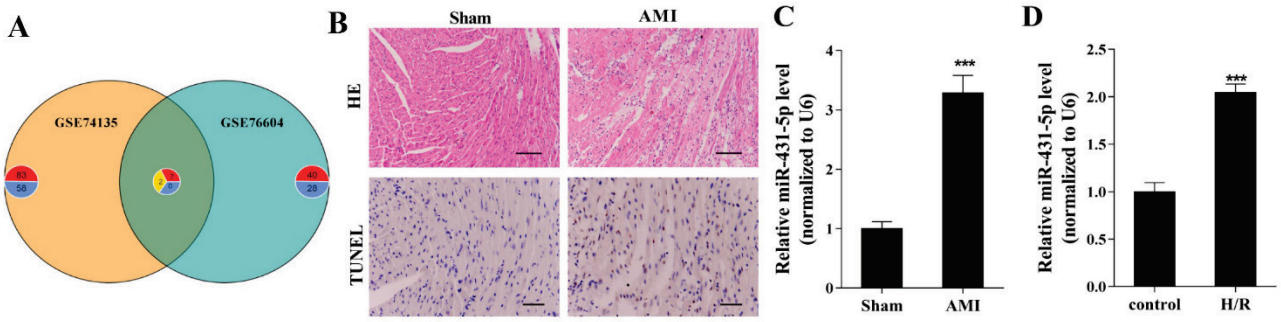

Fig. 1. The expression of miR-431-5p was elevated in AMI myocardial tissues and H/R-induced HL-1 cardiomyocytes. (**A**) NCBI GEO Datasets were used to select the candidate miRNAs. Red represents increased miRNA expression. Blue represents decreased miRNA expression. Yellow represents inconsistent miRNA expression. C57BL/6J male mice were used to establish a mouse model of AMI by ligating the left anterior descending branch of coronary artery. Animals were divided into the Sham group (n=5) and the AMI group (n=5). (**B**) H&E staining and TUNEL staining of mouse myocardial tissues. H&E staining (Scale bar=100 μm), TUNEL staining (Scale bar=40 μm). (**C**) qRT-PCR was performed to measure the expression of miR-431-5p in myocardial tissues. (**D**) The cardiomyocyte injury model was established by H/R treatment of HL-1 cells. HL-1 cells were grouped into the control group and the H/R group. qRT-PCR was performed to measure the expression of miR-431-5p in HL-1 cells induced by H/R treatment. *** P<0.001 vs. the Sham or control group.

Interference with miR-431-5p inhibited cardiomyocyte apoptosis in H/R-induced HL-1 cells

Next, to study the effect of miR-431-5p on cardiomyocyte apoptosis after AMI, the expression of miR-431-5p was inhibited by transfecting miR-431-5p antagomir into H/R-induced HL-1 cells. The results of qRT-PCR demonstrated that the expression of miR-431-5p was down-regulated in H/R-induced HL-1 cells after transfection of miR-431-5p antagomir, indicating that miR-431-5p was successfully interfered in HL-1 cells (Fig. 2A). In addition, the mRNA and protein expression of SELT were down-regulated after the H/R treatment, which were up-regulated by miR-431-5p antagomir (Fig. 2B), indicating that miR-431-5p might negatively regulate SELT expression in H/R induced HL-1 cells. TUNEL staining and flow cytometry revealed that cell apoptosis in the H/R+miR-431-5p antagomir group was decreased compared with the H/R+ antagomor-NC group (Fig. 2C). The expression of apoptosis-related proteins, cleaved-caspase 3, and Bax, was decreased, while the expression of Bcl-2 was increased (Fig. 2D). The results of MTT assay indicated that HL-1 cell viability was decreased after H/R treatment, which was increased significantly after interfering with miR-431-5p (Fig. 2E). The results of LDH assay indicated that LDH activity in the H/R+miR-431-5p antagomir group was significantly decreased compared with the H/R+antagomir-NC group (Fig. 2F).

Targeting relationship between miR-431-5p and SELT

To clarify the targeting relationship between miR-431-5p and SELT, we conducted a dual-luciferase reporter gene assay, and qRT-PCR and western blotting were performed to measure the mRNA and protein expression of SELT after interference or overexpression of miR-431-5p in HL-1 cells. Figure 3A showed the potential binding site between miR-431-5p and SELT by Targetscan (http://www.targetscan.org/mmu_72/). Compared with the antagomir-NC group, interfering miR-431-5p (miR-431-5p antagomir) increased the luciferase activity of the SELT 3' UTR-WT, and up-regulated the mRNA and protein expression of SELT (Fig. 3B). Overexpression of miR-431-5p (miR-431-5p agomir) inhibited the luciferase activity of SELT 3' UTR-WT and down-regulated the expression of mRNA and protein of SELT (Fig. 3C).

miR-431-5p affected cardiomyocyte apoptosis of H/R-induced HL-1 cells by targeting SELT

Finally, to further confirm the targeting relationship between miR-431-5p and SELT, miR-431-5p antagomir and si-SELT were transfected into HL-1 cells simultaneously. After 48 h of H/R treatment in HL-1 cells, we found that the simultaneous interference with miR-431-5p and SELT down-regulated the expression of SELT at both the mRNA and protein levels (Fig. 4A and 4B), up-regulated the expression of Bax and cleaved-caspase 3, and down-regulated Bcl-2 expression (Fig. 4B). Compared with interfering miR-431-5p alone, TUNEL staining and flow cytometry showed that cell apoptosis was increased (Fig. 4C) and MTT assay results indicated that cell viability was decreased after the simultaneous interference with miR-431-5p and SELT (Fig. 4D). LDH activity was increased after the simultaneous interference with miR-431-5p and SELT (Fig. 4E).

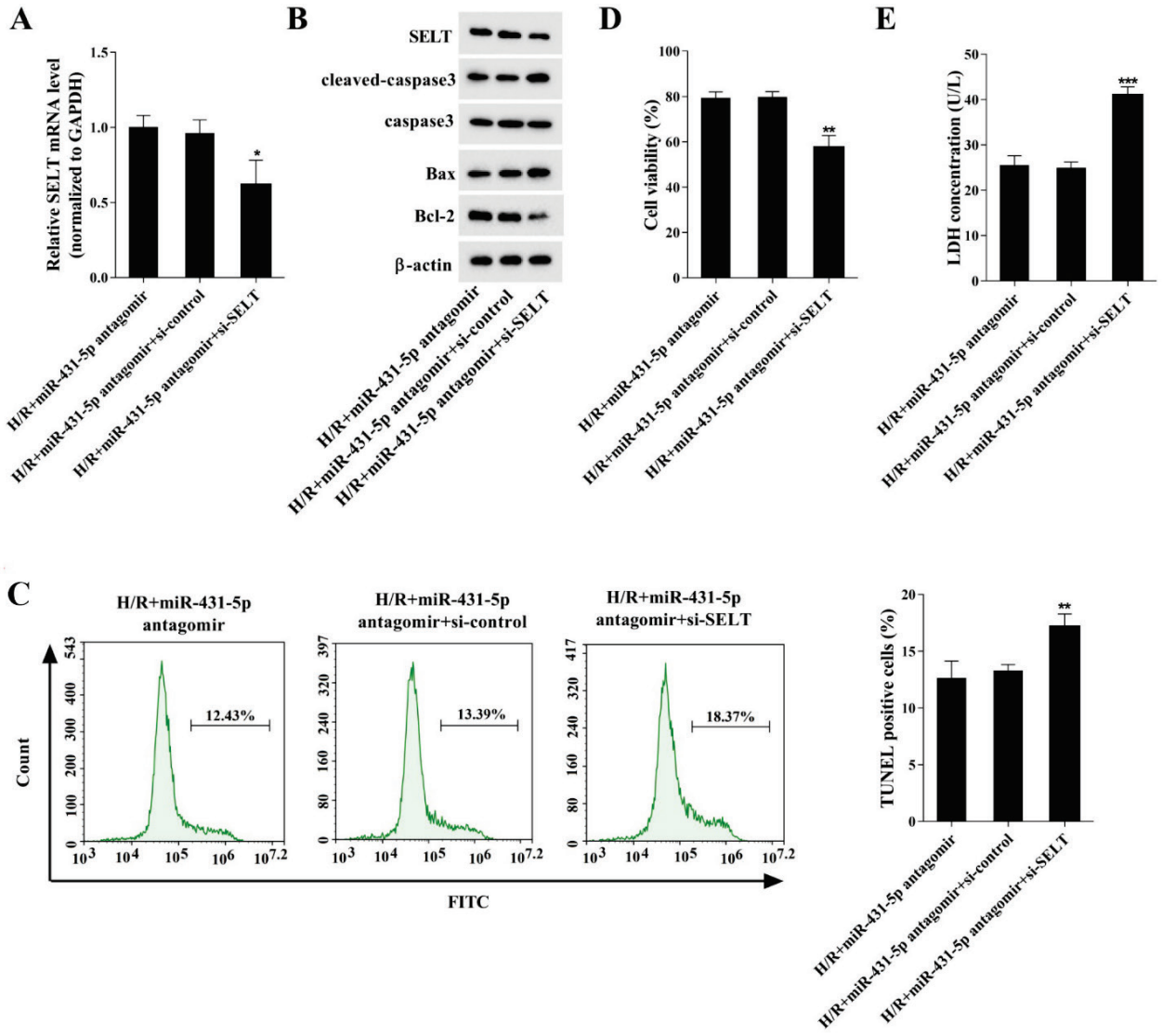

Fig. 2. Interference with miR-431-5p inhibited cardiomyocyte apoptosis in H/R-induced HL-1 cells. HL-1 cells were transfected with miR-431-5p antagomir or antagomir-NC. Cells were grouped into the control, H/R, H/R+antagomir-NC, and H/R+miR-431-5p antagomir group. (**A**) After 48 h of H/R treatment, the expression of miR-431-5p was detected by qRT-PCR. (**B**) After 48 h of H/R treatment, qRT-PCR and western blotting were performed to measure the mRNA and protein expression of SELT. (**C**) After 48 h of H/R treatment, TUNEL staining and flow cytometry was carried out to determine cell apoptosis. (**D**) After 48 h of H/R treatment, western blotting was performed to measure the expression of apoptotic proteins cleaved-caspase 3, Bcl-2, and Bax. (**E**) After 48 h of H/R treatment, MTT assay was carried out to examine cell viability. (**F**) After 48 h of H/R treatment, LDH activity was measured using an LDH cytotoxicity detection kit. ** P<0.01, *** P<0.001 vs. the control group, $^{\#}$ P<0.05, $^{\#\#}$ P<0.01, or $^{\#\#\#}$ P<0.001 vs. the H/R+antagomir-NC group.

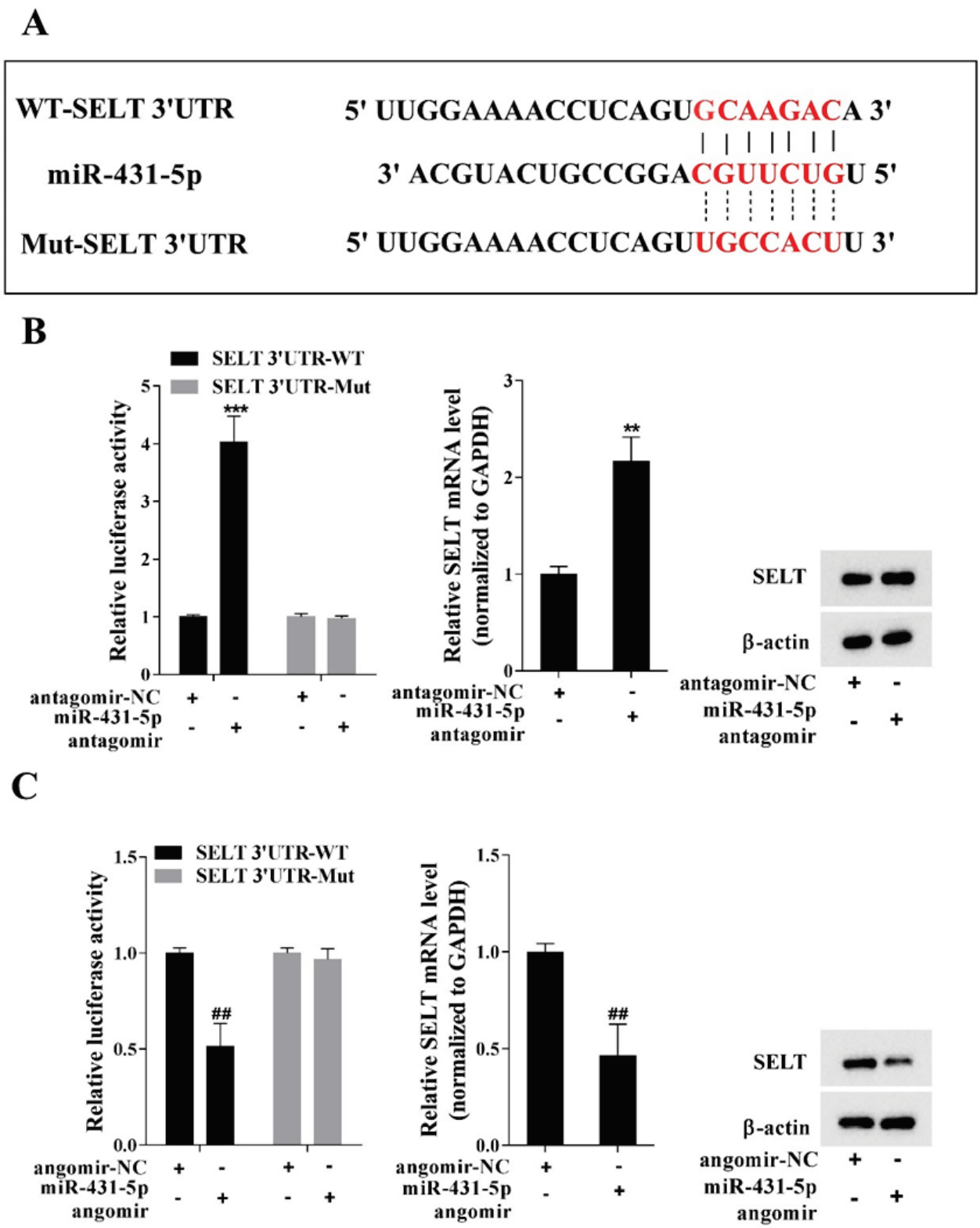

Fig. 3. Targeting relationship between miR-431-5p and SELT. (**A**) TargetScan database predicted that miR-431-5p bind to the 3′ UTR region of SELT mRNA. (**B**) HL-1 cells were transfected with SELT 3′ UTR-WT or SELT 3′ UTR-Mut, miR-431-5p antagomir, or antagomir-NC. The luciferase activity was measured by dual-luciferase reporter gene assay. qRT-PCR and western blotting were performed to measure the mRNA and protein expression of SELT, respectively. (**C**) HL-1 cells were transfected with SELT 3′ UTR-WT or SELT 3′ UTR-Mut, miR-431-5p agomir, or agomir-NC. The luciferase activity was measured by dual-luciferase reporter gene assay. qRT-PCR and western blotting were performed to measure the mRNA and protein expression of SELT, respectively. ** P<0.01, *** P<0.001 vs. the antagomir-NC group, $^{\#\#}$ P<0.01 vs. the agomir-NC group.

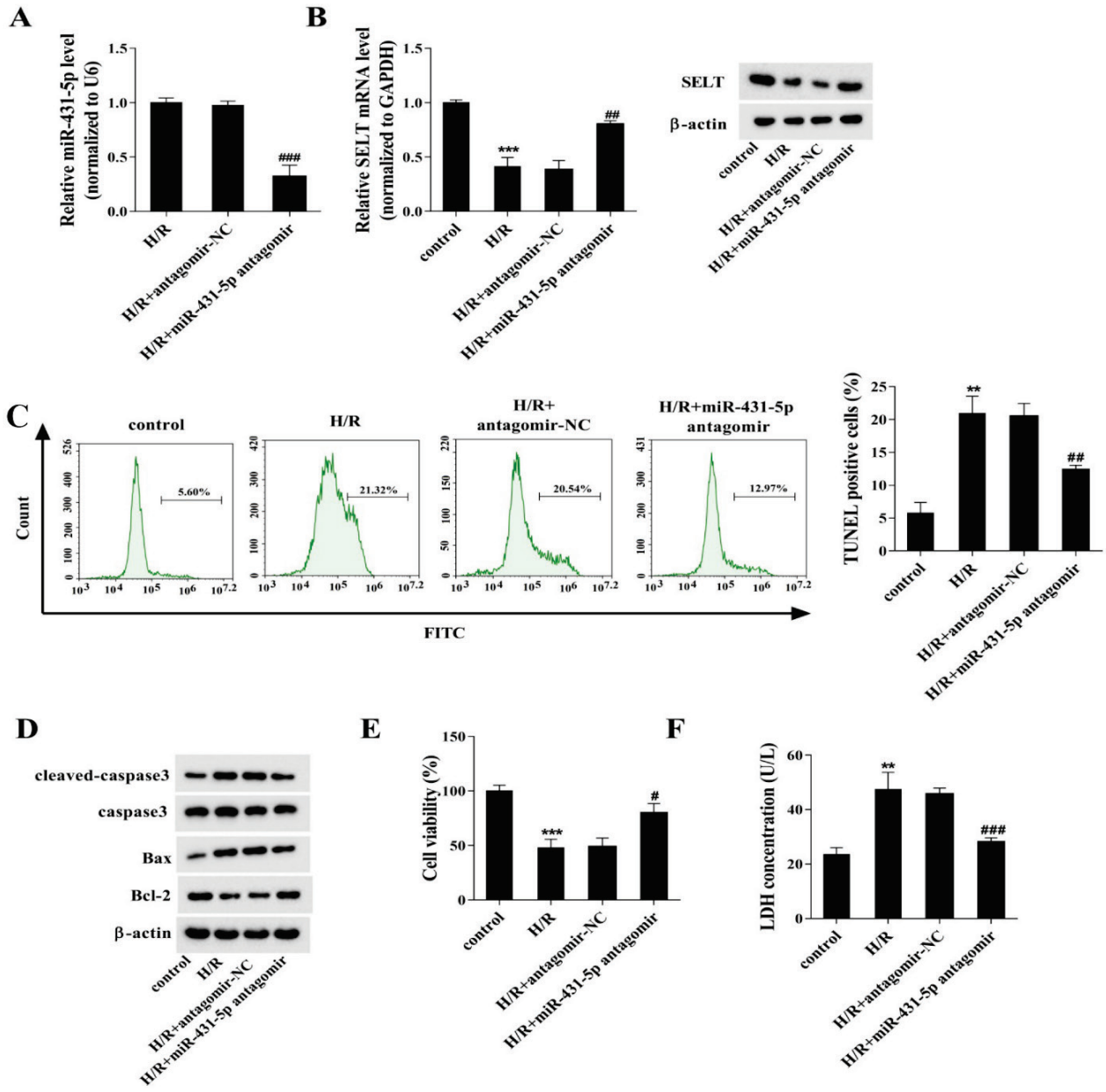

Fig. 4. miR-431-5p affected cardiomyocyte apoptosis of H/R-induced HL-1 cells by targeting SELT. HL-1 cells were transfected with miR-431-5p antagomir or co-transfected with miR-431-5p antagomir+si-SELT simultaneously. HL-1 cells were grouped into: H/R+miR-431-5p antagomir, H/R+miR-431-5p antagomir+si-control, and H/R+miR-431-5p antagomir+si-SELT group. (**A**) After 48 h of H/R treatment, qRT-PCR was performed to measure the expression of SELT mRNA. (**B**) After 48 h of H/R treatment, western blotting was performed to measure the protein expression of SELT, Bax, Bcl-2, and cleaved-caspase 3. (**C**) After 48 h of H/R treatment, TUNEL staining and flow cytometry was carried out to determine cell apoptosis. (**D**) After 48 h of H/R treatment, MTT assay was carried out to examine cell viability. (**E**) After 48 h of H/R treatment, LDH activity was measured using an LDH cytotoxicity detection kit. * P<0.05, ** P<0.01, *** P<0.001 vs. the H/R+miR-431-5p antagomir+si-control group.

Discussion

This study investigated the role of miR-431-5p in AMI for the first time. Also, it showed that miR-431-5p affected AMI by regulating cardiomyocyte apoptosis. The gain and loss of function experiments conducted in H/R-induced mouse cardiomyocyte cell line HL-1 proved that miR-431-5p affected cardiomyocyte apoptosis and viability through regulating SELT. Interfering with miR-431-5p up-regulated the expression of SELT, inhibited cardiomyocyte apoptosis, improved cardiomyocyte viability, and reduced cardiomyocyte damage, thereby providing its potential application value in the therapy of AMI.

miRNAs are small non-coding RNAs which can regulate gene expression at the post-transcriptional level

by inhibiting the translation of mRNA or promoting mRNA degradation. Various physiological processes and pathologies (including cancer, cardiovascular diseases, and metabolic diseases) are highly dependent on miRNAs [18]. Recently, extensive research has revealed the importance of miRNAs in AMI [19,20]. For example, Zheng *et al.* [21] found that miRNA-488-3p reduces LDH activity in AMI mice and down-regulates the expression of caspase 3 in mouse cardiomyocytes (MCM) by down-regulating ZNF791. Our study found that miR-431-5p was highly expressed in myocardial tissues of AMI mice and H/R-treated HL-1 cells. This result was consistent with the trend of miR-431-5p expression in atherosclerosis [22]. Through cell transfection experiments, we found that the apoptosis of HL-1 cells was reduced after interfering with miR-431-5p, and the expression of apoptosis-related proteins cleaved-caspase 3 and bax was down-regulated, and Bcl-2 expression was up-regulated. Moreover, by the interference with miR-431-5p, the viability of H/R-induced HL-1 cells was significantly increased. These data demonstrated that miR-431-5p was involved in cardiomyocyte apoptosis after AMI.

Selenium is an essential trace element for human body which is mainly involved in regulating various physiological links and exerting different biological functions in the form of selenoproteins and thus is directly or indirectly associated with a variety of major diseases [23]. Mammalian selenoprotein SELT has been reported to play a significant role in many diseases [24-27]. In addition, there is evidence that SELT protects myocardial tissues in cardiovascular diseases including myocardial ischemia-reperfusion injury [11,28]. In this study, we found lower expression of SELT in H/R-induced HL-1 cells. Through luciferase reporter gene assay and cell transfection experiments, SELT was confirmed to be one of the target genes of miR-431-5p, and the expression of SELT was negatively regulated by miR-431-5p. Interference or overexpression of miR-431-5p in HL-1 cells up-regulated or downregulated the expression of SELT, suggesting that miR-431-5p targeted SELT and negatively regulated its expression in AMI.

Cardiomyocytes are heart muscle cells, which are responsible for myocardial contraction [29,30]. The loss or death of cardiomyocytes in ischemic myocardial tissues seriously affects the recovery of heart function after AMI and is of great significance to the survival and long-term prognosis of patients with AMI [31-33]. This study revealed that interference with miR-431-5p inhibited cardiomyocyte apoptosis that was caused by H/R treatment. In addition, we confirmed that SEL regulation was one of the possible mechanisms of miR-431-5p action in cardiomyocytes. SELT is one of the many metabolic pathways involved in apoptosis. Here, we revealed that silencing SELT reversed the inhibition of cardiomyocyte apoptosis caused by miR-431-5p interference, as well as the increase of cell viability and the reduction of cell damage, indicating that miR-431-5p might regulate cardiomyocyte apoptosis through SELT in AMI.

In conclusion, this study demonstrated that miR-431-5p was involved in cardiomyocyte apoptosis after AMI. The regulation mechanism was closely related to the downstream target SELT, but further research is needed to reveal the details of this mechanism. These results help us to study the pathophysiological mechanism of AMI and provide a new idea for the treatment of AMI that miR-453-5p knockdown may protect cardiomyocytes from apoptosis and thereby myocardial injury in AMI patients.

Conflict of Interest

There is no conflict of interest.

Acknowledgements

This work was supported by the Applied Research Program of Nantong (No. MS12018039).

References

1. Roger VL, Go AS, Lloyd-Jones DM, Benjamin EJ, Berry JD, Borden WB, Bravata DM, Dai S, Ford ES, Fox CS, Fullerton HJ, Gillespie C, Hailpern SM, Heit JA, Howard VJ, Kissela BM, Kittner SJ, Lackland DT, Lichtman JH, Lisabeth LD, ET AL. Executive summary: heart disease and stroke statistics--2012 update: A report from the American Heart Association. Circulation 2012;125:188-197. https://doi.org/10.1161/CIR.0b013e3182456d46
2. Reed GW, Rossi JE, Cannon CP. Acute myocardial infarction. Lancet 2017;389:197-210. https://doi.org/10.1016/S0140-6736(16)30677-8

3. Lekkas P, Georgiou ES, Kontonika M, Mouchtouri ET, Mourouzis I, Pantos C, Kolettis TM. Intracerebroventricular endothelin receptor-A blockade in rats decreases phase-II ventricular tachyarrhythmias during acute myocardial infarction. Physiol Res 2019;68:867-871. https://doi.org/10.33549/physiolres.934135
4. Nichols M, Townsend N, Scarborough P, Rayner M. Cardiovascular disease in Europe 2014: Epidemiological update. Eur Heart J 2014;35:2950-2959. https://doi.org/10.1093/eurheartj/ehu299
5. Nazir S, Tachamo N, Lohani S, Hingorani R, Poudel DR, Donato A. Acute myocardial infarction and antiphospholipid antibody syndrome: A systematic review. Coron Artery Dis 2017;28:332-335. https://doi.org/10.1097/MCA.0000000000000476
6. Takemura G, Fujiwara H. Morphological aspects of apoptosis in heart diseases. J Cell Mol Med 2006;10:56-75. https://doi.org/10.1111/j.1582-4934.2006.tb00291.x
7. Anderson ME, Brown JH, Bers DM. CaMKII in myocardial hypertrophy and heart failure. J Mol Cell Cardiol 2011;51:468-473. https://doi.org/10.1016/j.yjmcc.2011.01.012
8. Gajarsa JJ, Kloner RA. Left ventricular remodeling in the post-infarction heart: a review of cellular, molecular mechanisms, and therapeutic modalities. Heart Fail Rev 2011;16:13-21. https://doi.org/10.1007/s10741-010-9181-7
9. Cong L, Su Y, Wei D, Qian L, Xing D, Pan J, Chen Y, Huang M. Catechin relieves hypoxia/reoxygenation-induced myocardial cell apoptosis via down-regulating lncRNA MIAT. J Cell Mol Med 2020;24:2356-2368. https://doi.org/10.1111/jcmm.14919
10. Wang Y, Ju C, Hu J, Huang K, Yang L. PRMT4 overexpression aggravates cardiac remodeling following myocardial infarction by promoting cardiomyocyte apoptosis. Biochem Biophys Res Commun 2019;520:645-650. https://doi.org/10.1016/j.bbrc.2019.10.085
11. Rocca C, Boukhzar L, Granieri MC, Alsharif I, Mazza R, Lefranc B, Tota B, Leprince J, Cerra MC, Anouar Y, Angelone T. A selenoprotein T-derived peptide protects the heart against ischaemia/reperfusion injury through inhibition of apoptosis and oxidative stress. Acta Physiol (Oxf) 2018;223:e13067. https://doi.org/10.1111/apha.13067
12. Cui Y, Bai Y, Wang XD, Liu B, Zhao Z, Wang LS. Differential expression of miRNA in rat myocardial tissues under psychological and physical stress. Exp Ther Med 2014;7:901-906. https://doi.org/10.3892/etm.2014.1504
13. Zhou SS, Jin JP, Wang JQ, Zhang ZG, Freedman JH, Zheng Y, Cai L. miRNAS in cardiovascular diseases: potential biomarkers, therapeutic targets and challenges. Acta Pharmacol Sin 2018;39:1073-1084. https://doi.org/10.1038/aps.2018.30
14. Wang C, Jing Q. Non-coding RNAs as biomarkers for acute myocardial infarction. Acta Pharmacol Sin 2018;39:1110-1119. https://doi.org/10.1038/aps.2017.205
15. Huo KG, Richer C, Berillo O, Mahjoub N, Fraulob-Aquino JC, Barhoumi T, Ouerd S, Coelho SC, Sinnett D, Paradis P, Schiffrin EL. miR-431-5p knockdown protects against angiotensin II-induced hypertension and vascular injury. Hypertension 2019;73:1007-1017. https://doi.org/10.1161/HYPERTENSIONAHA.119.12619
16. Rapa I, Votta A, Felice B, Righi L, Giorcelli J, Scarpa A, Speel EJ, Scagliotti GV, Papotti M, Volante M. Identification of microRNAs differentially expressed in lung carcinoid subtypes and progression. Neuroendocrinology 2015;101:246-255. https://doi.org/10.1159/000381454
17. Li H, Tang C, Zhu X, Zhang W, Abudupataer M, Ding S, Duan C, Yang X, Ge J. Histamine deficiency facilitates coronary microthrombosis after myocardial infarction by increasing neutrophil-platelet interactions. J Cell Mol Med 2020;24:3504-3520. https://doi.org/10.1111/jcmm.15037
18. Correia de Sousa M, Gjorgjieva M, Dolicka D, Sobolewski C, Foti M. Deciphering miRNAs' action through miRNA editing. Int J Mol Sci 2019;20:6249. https://doi.org/10.3390/ijms20246249
19. Boon RA, Dimmeler S. MicroRNAs in myocardial infarction. Nat Rev Cardiol 2015;12:135-142. https://doi.org/10.1038/nrcardio.2014.207
20. Chen Y, Zhao Y, Chen W, Xie L, Zhao ZA, Yang J, Chen Y, Lei W, Shen Z. MicroRNA-133 overexpression promotes the therapeutic efficacy of mesenchymal stem cells on acute myocardial infarction. Stem Cell Res Ther 2017;8:268. https://doi.org/10.1186/s13287-017-0722-z
21. Zheng HF, Sun J, Zou ZY, Zhang Y, Hou GY. MiRNA-488-3p suppresses acute myocardial infarction-induced cardiomyocyte apoptosis via targeting ZNF791. Eur Rev Med Pharmacol Sci 2019;23:4932-4939. https://doi.org/10.26355/eurrev_201906_18083

22. Aavik E, Lumivuori H, Leppänen O, Wirth T, Häkkinen SK, Bräsen JH, Beschorner U, Zeller T, Braspenning M, van Criekinge W, Mäkinen K, Ylä-Herttuala S. Global DNA methylation analysis of human atherosclerotic plaques reveals extensive genomic hypomethylation and reactivation at imprinted locus 14q32 involving induction of a miRNA cluster. Eur Heart J 2015;36:993-1000. https://doi.org/10.1093/eurheartj/ehu437
23. Moghadaszadeh B, Beggs AH. Selenoproteins and their impact on human health through diverse physiological pathways. Physiology (Bethesda) 2006;21:307-315. https://doi.org/10.1152/physiol.00021.2006
24. Prevost G, Arabo A, Jian L, Quelennec E, Cartier D, Hassan S, Falluel-Morel A, Tanguy Y, Gargani S, Lihrmann I, Kerr-Conte J, Lefebvre H, Pattou F, Anouar Y. The PACAP-regulated gene selenoprotein T is abundantly expressed in mouse and human β-cells and its targeted inactivation impairs glucose tolerance. Endocrinology 2013;154:3796-3806. https://doi.org/10.1210/en.2013-1167
25. Castex MT, Arabo A, Bénard M, Roy V, Le Joncour V, Prévost G, Bonnet JJ, Anouar Y, Falluel-Morel A. Selenoprotein T deficiency leads to neurodevelopmental abnormalities and hyperactive behavior in mice. Mol Neurobiol 2016;53:5818-5832. https://doi.org/10.1007/s12035-015-9505-7
26. Boukhzar L, Hamieh A, Cartier D, Tanguy Y, Alsharif I, Castex M, Arabo A, El Hajji S, Bonnet JJ, Errami M, Falluel-Morel A, Chagraoui A, Lihrmann I, Anouar Y. Selenoprotein T exerts an essential oxidoreductase activity that protects dopaminergic neurons in mouse models of Parkinson's disease. Antioxid Redox Signal 2016;24:557-574. https://doi.org/10.1089/ars.2015.6478
27. Huang J, Bao D, Lei CT, Tang H, Zhang CY, Su H, Zhang C. Selenoprotein T protects against cisplatin-induced acute kidney injury through suppression of oxidative stress and apoptosis. FASEB J 2020;34:11983-11996. https://doi.org/10.1096/fj.202000180RR
28. Rocca C, Pasqua T, Boukhzar L, Anouar Y, Angelone T. Progress in the emerging role of selenoproteins in cardiovascular disease: focus on endoplasmic reticulum-resident selenoproteins. Cell Mol Life Sci 2019;76:3969-3985. https://doi.org/10.1007/s00018-019-03195-1
29. Torrealba N, Navarro-Marquez M, Garrido V, Pedrozo Z, Romero D, Eura Y, Villalobos E, Roa JC, Chiong M, Kokame K, Lavandero S. Herpud1 negatively regulates pathological cardiac hypertrophy by inducing IP3 receptor degradation. Sci Rep 2017;7:13402. https://doi.org/10.1038/s41598-017-13797-z
30. Bildyug N. Extracellular matrix in regulation of contractile system in cardiomyocytes. Int J Mol Sci 2019;20:5054. https://doi.org/10.3390/ijms20205054
31. Chen T, Zhu H, Wang Y, Zhao P, Chen J, Sun J, Zhang X, Zhu G. Apoptosis of bone marrow mesenchymal stromal/stem cells via the MAPK and endoplasmic reticulum stress signaling pathways. Am J Transl Res 2018;10:2555-2566. https://doi.org/10.1155/2018/9501747
32. Meng K, Jiao J, Zhu RR, Wang BY, Mao XB, Zhong YC, Zhu ZF, Yu KW, Ding Y, Xu WB, Yu J, Zeng QT, Peng YD. The long noncoding RNA hotair regulates oxidative stress and cardiac myocyte apoptosis during ischemia-reperfusion injury. Oxid Med Cell Longev 2020;2020:1645249. https://doi.org/10.1155/2020/1645249
33. Gao X, Zhang S, Wang D, Cheng Y, Jiang Y, Liu Y. (Pro)renin receptor contributes to hypoxia/reoxygenation-induced apoptosis and autophagy in myocardial cells via the beta-catenin signaling pathway. Physiol Res 2020;69:427-438. https://doi.org/10.33549/physiolres.934210